CHEMICAL ENGINEERING TRANSACTIONS
VOL. 114, 2024
A publication of AIDIC
The Italian Association of Chemical Engineering
Online at www.cetjournal.it
Guest Editors: Petar S. Varbanov, Min Zeng, Yee Van Fan, Xuechao Wang

ISBN 979-12-81206-12-0; **ISSN** 2283-9216
DOI: 10.3303/CET24114138

Advanced Numerical Simulation and Modeling of Multi-Pass Welding Processes: Detailed Analysis of Temperature Distribution in Structural Elements

Dániel Gosztola*, Péter Grubits, János Szép, Majid Movahedi Rad

Faculty of Architecture, Civil Engineering and Transport Sciences, Department of Structural and Geotechnical Engineering, Széchenyi István University, H-9026 Győr, Hungary
gosztola.daniel@sze.hu

The growing importance of numerical simulations in the welding industry stems from their ability to enhance structural performance and sustainability by ensuring optimal manufacturing conditions. The use of the finite element method (FEM) allows for detailed and precise calculations of the mechanical and material changes caused by the welding process. Acquiring knowledge of these parameters not only serves to augment the quality of the manufacturing process but also yields consequential benefits, such as reducing adverse effects. Consequently, the enhancement of structural performance and prolonged lifespan becomes achievable, aligning with overarching sustainability goals. To achieve this goal, this paper utilizes numerical simulations of welding processes based on experimental tests, with a specific focus on analyzing temperatures generated within the structures. In the finite element analysis (FEA), a total of 12 welding cycles were systematically modeled to align with experimental conditions, incorporating cooling intervals, preheating considerations, and the relevant section of the connecting concrete structure with studs. The outcomes of this research exemplify the potential of numerical simulation in the welding industry, demonstrating a diverse range of results achieved through FEA to enhance the quality of structures within the context of sustainability.

1. Introduction

The groundbreaking work of Goldak et al. (1992) made a substantial early contribution to welding modeling by analyzing microstructure evolution, integrating heat transmission, and thermal stress analysis. Ueda and Yamakawa (1971) developed a method for theoretical analysis that considered variations in temperature distribution over time and their impact on the mechanical properties of materials, marking an important milestone in the field. Despite these advancements, significant knowledge gaps remain in understanding the complex thermal and mechanical interactions during multi-pass welding, particularly in relation to the impact on structural integrity and long-term performance.

Recent studies have continued to expand on these early developments. Habashneh et al. (2023, 2024) emphasized the critical role of ambient temperature variations on structural behavior. Similarly, studies by Deng et al. (2007) and Zhao et al. (2018) have utilized Finite Element Analysis (FEA) to simulate welding processes, focusing on inherent strain theory and the design of welding structures. However, many of these studies either focus on single-pass welding or do not fully explore the impact of multi-pass welding on connected structures, particularly in complex environments involving dissimilar materials like steel and concrete. For instance, while Wang et al. (2013) and Zubairuddin et al. (2017) investigated multi-pass welding, their focus was primarily on residual stresses and distortion without a comprehensive assessment of temperature-induced effects on interconnected materials.

This study aims to address this gap by focusing specifically on the multi-pass welding process and its thermomechanical impact on connected structures, such as steel plates and concrete blocks. The approach presented simulates a 12-cycle multi-pass welding process involving two 20 mm steel plates and incorporates a connecting concrete block to replicate experimental conditions and provide validation. An advanced

Paper Received: 25 May 2024; Revised: 16 July 2024; Accepted: 20 November 2024
Please cite this article as: Gosztola D., Grubits P., Szép J., Rad M.M., 2024, Advanced Numerical Simulation and Modeling of Multi-Pass Welding Processes: Detailed Analysis of Temperature Distribution in Structural Elements, Chemical Engineering Transactions, 114, 823-828 DOI:10.3303/CET24114138

thermomechanical analysis framework is employed to evaluate the temperature distribution and its influence on the structure.
The novelty of this study lies in its comprehensive approach to simulating and validating the complex interactions between welded steel and adjacent materials, such as concrete, in a multi-pass welding process. This provides a more realistic and applicable understanding of how welding-induced heat affects structural integrity. The relevance of this work is underscored by the growing need for durable, long-lasting infrastructure, where welding processes play a crucial role in the assembly and maintenance of structural components.

2. Finite element modeling and welding analysis

2.1 Thermal analysis

The conservation of energy is the fundamental principle underlying thermal analysis. Heat transfer theory was applied to simulate the welding process by calculating the temperature evolution at each individual node. The concept is based on the flux of energy, which is described by Eq(1) (Goldak and Akhlaghi, 2005), where q represents the heat flux, proportional to the thermal conductivity κ and the temperature gradient ∇T.

$$q = -\kappa \nabla T \tag{1}$$

With the use of the heat conduction formula Eq(2) (Goldak and Akhlaghi, 2005) and the knowledge of q, it is possible to determine the temperature in each node. The density of the material is represented by ρ in this equation, together with the specific heat capacity c_p, temperature T, heat flux vector q, heat generation term Q, time t, and spatial gradient operator Δ.

$$\frac{\rho c_p dT}{dt} + \nabla(-\kappa \nabla T) + Q = 0 \tag{2}$$

The increment in specific enthalpy under constant pressure due to a small temperature change is expressed in Eq(3) (Goldak and Akhlaghi, 2005).

$$dh = c_p dT \tag{3}$$

where dT is the temperature increase and c_p is the specific heat capacity.
The double ellipsoidal heat source model, which was developed by Goldak et al. (1984) and is frequently used for arc welding, was used in this study to simulate the heat produced during welding, as shown in Eq(4) and (5). The power density distribution q in the front and rear quadrants is identified as follows:

$$Q(x,y,z,t) = \frac{6\sqrt{3} f_f Q_w}{abc\pi\sqrt{\pi}} e^{-3x^2/a^2} e^{-3y^2/b^2} e^{-3z^2/{c_f}^2} \tag{4}$$

$$Q(x,y,z,t) = \frac{6\sqrt{3} f_r Q_w}{abc\pi\sqrt{\pi}} e^{-3x^2/a^2} e^{-3y^2/b^2} e^{-3z^2/{c_r}^2} \tag{5}$$

where the parameters a, b, and c, which represent the different axes of the ellipsoid aligned with the coordinates x, y, and z, respectively, determine the width, depth, and length of the welding pool. f_r and f_f represent the fraction factors of the heat, where $f_r + f_f = 2$ (Goldak et al., 1984), Q_w denotes the energy input, identified as follows:

$$Q_w = \eta U I \tag{6}$$

where *η* signs the efficiency of the procedure, *U* is voltage, and *I* signs the welding current. The parameters utilized for the simulation are presented in Table 1.

Table 1: Utilized parameters

Parameter	Value	Unit
Depth of the heat source	2.00	mm
Width of the heat source	2.00	mm
Front length	2.50	mm
Rear length	5.00	mm
U	23.00	V
η	0.60	-
I	260.00	A

The differential equation presented in Eq(1) may be resolved through the specification of appropriate boundary conditions. This principle is exemplified in Eq(6) as outlined by Goldak et al. (1984). In this equation, T_0 represents the ambient temperature accounting for convection and radiation effects, κ denotes the thermal conductivity normal to the surface, σ responds the Stefan-Boltzmann constant, ε signifies the emissivity, q denotes the supplied flux, and h represents the convective heat transfer coefficient.

$$\kappa_n \frac{dT}{dn} + q + h(T - T_0) + \sigma\varepsilon\left(T^4 - {T_0}^4\right) = 0 \tag{7}$$

The variables employed in the simulation are enumerated in Table 2.

Table 2: Parameters for thermal properties

Coefficient	Value	Unit
Thermal conductivity normal to the surface	20	W/mK
Coefficient for emission	0.60	-
Coefficient for convection	100	W/m^{2}K

2.2 Mechanical analysis principles

Expansion and contraction are induced by variations in heat distribution between the region immediately adjacent to the welding spot and the surrounding areas. This thermal gradient results in significant stresses due to the material's thermal strains (Anca et al., 2011). The accurate computation of nonlinear deformation in simulations necessitates the integration of geometric compatibility, constitutive stress-strain relations, and equilibrium equations. The displacement field is interpolated over the element utilizing the von Mises yield criterion and a standard elastoplastic material model (Lindgren, 2007).

$$^{n+1}_{i}u(^{n+1}_{i}x, t) = N_m(^{n+1}_{i}x)^{n+1}_{i}u(t) \tag{8}$$

where $^{n+1}_{i}u(t)$ indicates the current estimation of the element displacement vector following completion of the increment and $^{n+1}_{i}x$ is its corresponding coordinate. $N_m(^{n+1}_{i}x, t)$ is the matrix containing the interpolation and shape function.

2.3 Finite element modeling and analysis

To comprehensively investigate the structural behavior and conduct detailed analysis, a complete 3D model was developed, as illustrated in Figure 1. This model represents a critical segment of the experimental setup, featuring the flange plate (red) measuring 300x80x20 mm and the stud plate (green) measuring 320x80x20 mm from a steel-concrete composite bridge. Additionally, it includes studs (blue) and a concrete block (grey) measuring 700x80x300 mm. To accurately simulate structural behavior and model realistic boundary conditions, a section of the web plate was also incorporated into the model.

This model currently applies to this assembly with its specific structural dimensions; however, we intend to investigate modeling variations in weld types and materials, as well as their geometry and layout, with a focus on the analysis of distortions and stresses within the structure resulting from welding in further research.

In the simulation, both the flange plate and the stud plate were welded on both sides of an 80 mm-long section. The weld pool was sequentially formed in six steps as prescribed, resulting in an overall dimension of 8 mm, as depicted in Figure 1. Furthermore, validation points used to measure resulting temperatures during both numerical and experimental tests are marked in Figure 1. Point "A" is designated for validating the temperature of the steel plates, while point "B" is designated for the concrete.

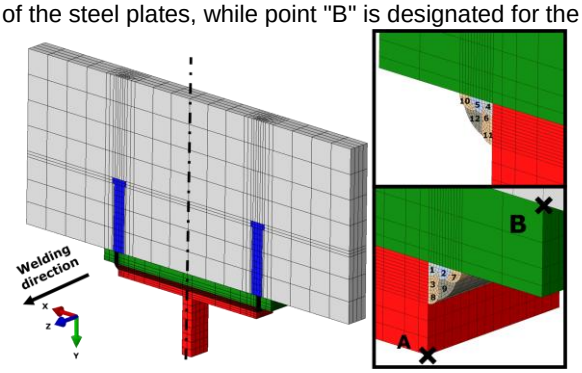

Figure 1: 3D Finite Element Model of the Assembly

ABAQUS software was utilized to conduct the simulation, which involved utilizing a combined temperature-displacement analysis. (Smith, 2009) This method integrates mechanical and thermal solutions concurrently, highlighting the critical importance of maintaining consistent element types and degrees of freedom throughout the study. Accordingly, a 3D thermally coupled 8-node brick finite element with reduced integration (C3D8RT) was utilized to establish the presented model.

3. Results

3.1 Validation of temperature measurements

In the initial phase of the study, the primary objective was to validate the temperatures observed during experimental testing. To optimize the quality of the weld pool and achieve the most effective connection possible, these components were preheated to 100 °C. Considering the welding stages and the total welding time, the simulation lasted 723 s, including the corresponding cooling phase.
To achieve the main goal of this research phase, the temperature distribution at designated point "A," as depicted in Figure 1, was evaluated to validate the temperatures in the steel plates. The results, presented in Figure 2, demonstrate a close agreement between the temperatures predicted by the model and those observed in the experiment. Upon detailed analysis, the highest temperature recorded during the simulation was 208 °C, reflecting a deviation of only 4% from the experimental findings, which was determined by calculating the difference between the two values.

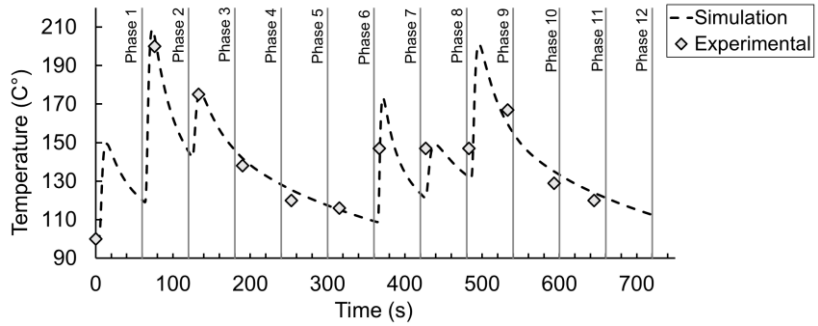

Figure 2: Temperature values recorded at measurement point A

Subsequently, the temperature evolution at point B, situated within the concrete, was derived from the simulation and compared to the experimental test results. The findings consistently fell within the acceptable margin of error, with the largest difference observed at approximately 4 %, as illustrated in Figure 3. This difference was calculated based on the variation between the two values.

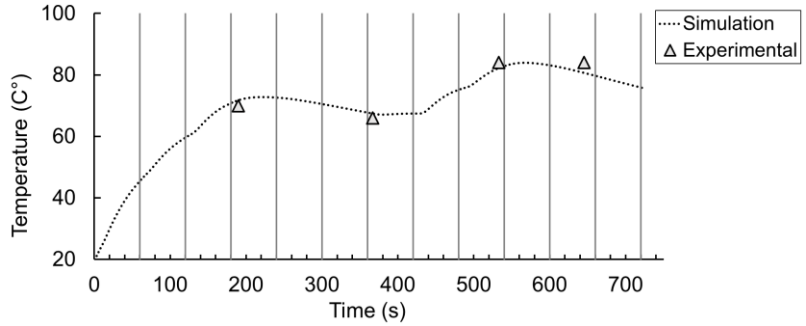

Figure 3: Temperature values recorded at measurement point B

3.2 Detailed temperature analysis of the concrete

In the second phase of the study, the primary objective was to analyze the temperature generated by the welding process in the concrete. Consequently, temperature values within the concrete block, which were inaccessible during experimental testing, were examined. As expected, the results illustrate a significant transfer of heat to the concrete by the steel components, with temperatures reaching a peak of approximately 107 °C at the bottom

section of the studs, as depicted in Figure 4. Building on the pioneering work of Shen and Xu (2019), it is evident that such temperatures can impact the mechanical properties of concrete. Therefore, for configurations akin to those studied here, ensuring optimal welding conditions and meticulously designing the welding process are crucial.

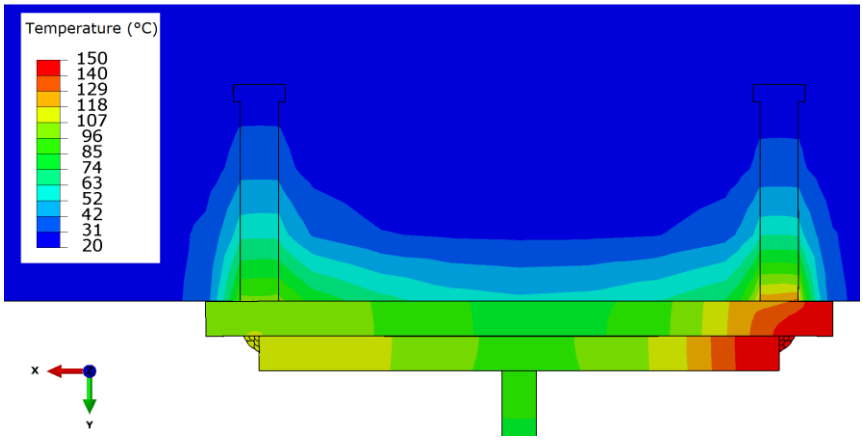

Figure 4: Temperature values at the end of the simulation

4. Conclusions

In this research, a detailed 3D numerical model was developed to analyze temperatures generated by welding processes, incorporating both steel and concrete components. A comprehensive thermal stress analysis encompassed 12 welding phases, cooling intervals, and temperature-dependent material properties. The model's accuracy was validated through experimental tests, measuring temperatures in both steel plates and concrete. The maximum observed deviation was approximately 5 % for steel plates and 4 % for concrete.
Additionally, in the second phase of the study, temperatures were investigated in concrete locations that were inaccessible during experimental tests. The results underscored the significant influence of welding processes on the structural properties of concrete, emphasizing its sensitivity to temperature changes.
This research establishes a robust foundation for advancing welding process performance through advanced numerical modeling. Furthermore, it provides crucial insights into how these processes can impact thermal dynamics in concrete, potentially influencing its structural integrity. The temperatures that developed in the cross member as a result of welding can be monitored throughout the welding process. The welded connection is a suitable method for joining components in steel-concrete composite bridges, and it is also applicable in scenarios where welding is necessary in close proximity to other materials, such as concrete.
Elevated temperatures can substantially alter the mechanical behavior of adjacent materials. Specifically, in the case of concrete, a reduction of 5-10 % in tensile and compressive strength may occur at temperatures exceeding 100 °C. In subsequent research, we aim to address the modeling of thermal effects on concrete, as well as the residual stresses and distortions.

Acknowledgments

Prepared with the professional support of the Doctoral Student Scholarship Program of the Co-operative Doctoral Program of the Ministry of Culture and Innovation financed from the National Research, Development and Innovation fund.

References

Anca A., Cardona A., Risso J., Fachinotti V.D., 2011, Finite element modeling of welding processes. Appl Math Model, 35, 688–707.
Deng D., Murakawa H., Liang W., 2007, Numerical simulation of welding distortion in large structures. Comput Methods Appl Mech Eng, 196, 4613–4627.
Goldak J.A., Akhlaghi M., 2005. Computational Welding Mechanics. Kluwer Academic Publishers, Boston, United States, DOI: 10.1007/b101137, ISBN: 978-0-387-23287-4.
Goldak J., Chakravarti A., Bibby M., 1984, A new finite element model for welding heat sources. Metallurgical Transactions B, 15, 299–305.

Goldak J., Oddy A., Gu M., Ma W., Mashaie A., Hughes E., 1992, Coupling Heat Transfer, Microstructure Evolution and Thermal Stress Analysis in Weld Mechanics. IUTAM Symposium on the Mechanical Effects of Welding, Springer, DOI: 10.1007/978-3-642-84731-8_1.

Grubits P., Gosztola D., Habashneh M., Szép J., Rad M.M., 2023, Advanced Numerical Simulation and Modeling of Welding Processes: Stochastic Representation of Parameters for Improved Fabrication. Chem. Eng. Trans., 107, 619–24, DOI: 10.3303/CET23107104.

Habashneh M., Rad M.M., 2023, Reliability based topology optimization of thermoelastic structures using bi-directional evolutionary structural optimization method. International Journal of Mechanics and Materials in Design, 19, 605–620, DOI: 10.1007/s10999-023-09641-0.

Habashneh M., Cucuzza R., Domaneschi M., Movahedi R. M., 2024, Advanced elasto-plastic topology optimization of steel beams under elevated temperatures. Advances in Engineering Software, 190, DOI: 10.1016/j.advengsoft.2024.103596.

Kollár D., Kövesdi B., Néző J., 2017, Numerical Simulation of Welding Process – Application in Buckling Analysis. Periodica Polytechnica, Civil Engineering, 61 98–109. URL: https://pp.bme.hu/ci/article/view/9257.

Lindgren L.-E., 2007. Computational welding mechanics: thermomechanical and microstructural simulations, Woodhead Publishing in materials. Woodhead, Cambridge, United Kingdom.

Shen J., Xu Q., 2019, Effect of elevated temperatures on compressive strength of concrete. Construction and Building Materials, 229, 1, 116846, DOI: 10.1016/j.conbuildmat.2019.116846.

Smith M., 2009, ABAQUS/Standard User's Manual, Version 6.9, Dassault Systèmes Simulia Corp., Providence, RI, United States.

Ueda Y., Yamakawa T., 1971, Analysis of Thermal Elastic-Plastic Stress and Strain During Welding by Finite Element Method. Transactions of the Japan Welding Society, 2, 90–100.

Wang Y., Wang L., Di X., Shi Y., Bao X., Gao X., 2013, Simulation and analysis of temperature field for in-service multi-pass welding of a sleeve fillet weld. Computational Materials Science, 68, 198–205, DOI: 10.1016/j.commatsci.2012.10.025.

Zhao S, Sun Y, Zhou Y, Yang W, Xie L, 2018, Friction Stir Welding Process and Chemical Properties Analysis of AZ80 Magnesium Alloy Material. Chem. Eng. Trans., 66, 691–696.

Zubairuddin M., Albert S.K., Vasudevan M., Mahadevan S., Chaudhari V., Suri V.K., 2017, Numerical simulation of multi-pass GTA welding of grade 91 steel. Journal of Manufacturing Process, 27, 87–97, DOI: 10.1016/j.jmapro.2017.04.031.